Rigid, Vapor-Permeable Poly(4-methyl-2-pentyne) Templates for High Resolution Patterning of Nanoparticles and Polymers

Michael T. Demko,[†,‡,*] Jim C. Cheng,[†,§] and Albert P. Pisano[†,‡,§]

[†]Berkeley Sensor & Actuator Center (BSAC), [‡]Department of Mechanical Engineering, and [§]Department of Electrical Engineering & Computer Sciences, University of California at Berkeley, Berkeley, California 94720, United States

ABSTRACT

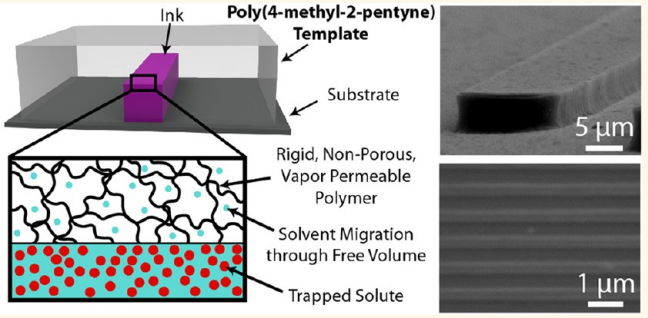

Soft lithography methods are emerging as useful tools for high-resolution, three-dimensional patterning of polymers and nanoparticles. However, the low Young's modulus of the standard template material, poly(dimethylsiloxane) (PDMS), limits attainable resolution, fidelity, and alignment capability. While much research has been performed to find other more rigid polymer template materials, the high solvent and vapor permeability that is characteristic of PDMS is often sacrificed, preventing their use in those processes reliant on this property. In this work, a highly rigid, chemically robust, optically transparent and vapor-permeable poly(4-methyl-2-pentyne) template is developed. The combination of high rigidity and high vapor permeability enables high resolution patterning with simplified ink handling. This material was nanopatterned to create a template for patterning polymers and nanoparticles, achieving a resolution of better than 350 nm.

KEYWORDS: polymeric materials · nanoparticles · patterning · poly(4-methyl-2-pentyne) · soft lithography · microfluidic molding

The choice of template material for use in patterning nanoparticles and polymers is critical to the ultimate resolution, fidelity, and registration capability of the resulting features. In the case of soft lithographic techniques such as nanoimprint lithography (NIL),[1] micromolding in capillaries (MIMIC),[2] solvent assisted micromolding (SAMIM),[3] solvent absorption micromolding,[4] and microfluidic molding (MM),[5] the elastomer poly(dimethylsiloxane) (PDMS) remains the material of choice for the templates. However, the low elasticity of PDMS has led to a substantial research effort into alternative template materials such as h-PDMS,[6] polyacrylates,[7] polyolefins,[8] polycarbonates,[9] polyurethanes,[10] and various fluoropolymers such as Dupont Teflon AF 2400[11] and PFPE.[12] However, with the exception of h-PDMS, which provides only a modest increase in the Young's modulus at the expense of higher susceptibility to brittle fracture, all such alternative polymers sacrifice the high vapor and solvent permeability that is characteristic of PDMS. This solvent permeability is critical to solvent-assisted micromolding, solvent absorption micromolding and microfluidic molding, and solvent and gas permeability is beneficial to applications of nanoimprint lithography and micromolding in capillaries where solvents and trapped gases must escape through the template.[1,2,13,14] As shown in Figure 1, separation of the solvent from the solutes in an ink by permeation is a simple method by which reflow of ink can be prevented once the template is removed from the substrate.[1,3−5] Solidification by solvent depletion avoids energy intensive thermal processing and eliminates the need for chemical modifications of the ink, including polymer binders and cross-linkers, which can modify the properties of the patterned material.[2,15,16] Such permeation can also be used to completely fill template features with concentrated solutes, resulting in three-dimensional patterning, or to fill templates in a completely additive manner, reducing material waste and eliminating energy intensive etching processes.[5]

For instances in which solvent or vapor permeability is required, the templates must allow passage of solvent molecules while

* Address correspondence to demko@berkeley.edu.

Received for review April 19, 2012 and accepted July 13, 2012.

Published online July 14, 2012
10.1021/nn3017266

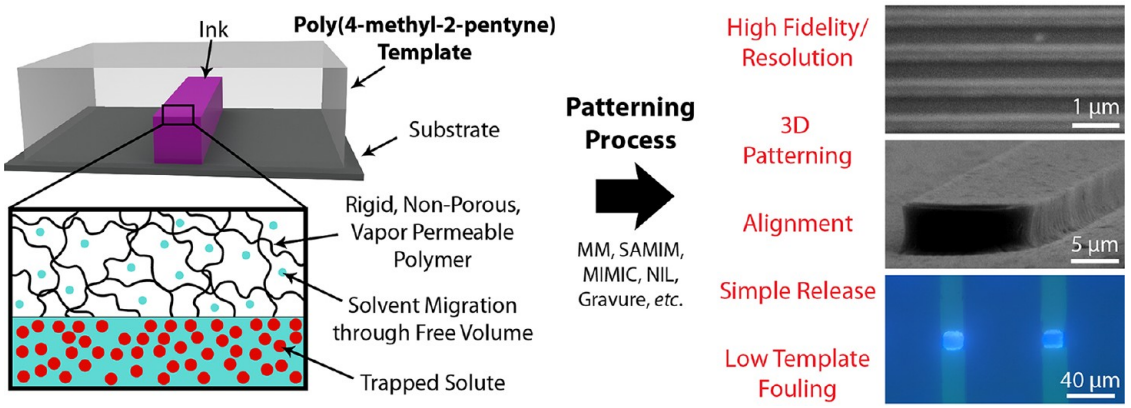

Figure 1. PMP as a template material. This rigid, polymer derives its vapor permeability from a high fractional free volume rather than explicit porosity. Solvents can permeate through the free volume of the polymer, while solutes are trapped in the template features. Together with high rigidity, high transparency, and low surface energy, this material can be used in a variety of patterning processes to achieve high feature quality.

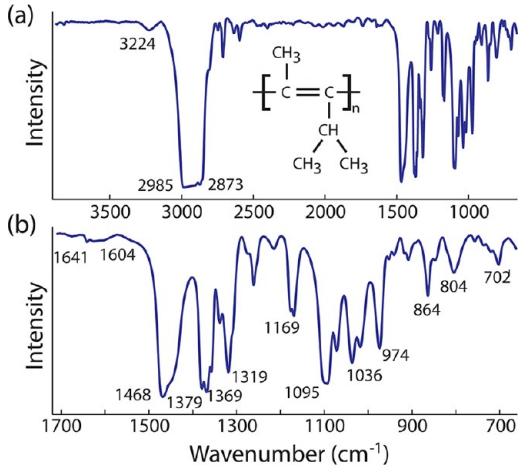

Figure 2. FT-IR spectrum of synthesized PMP. (a) The entire spectrum, with the chemical structure of PMP shown in the inset. (b) A magnified view of the "fingerprint" region of the spectrum.

blocking solutes. Explicitly porous materials are not desired since, given the extremely small size of certain nanoparticles or macromolecules, the surface of the template would be prone to fouling if any pores are larger than the critical dimension of the solute material, resulting in degraded performance over time. Rather, the vapor permeability should be the result of a high fractional free volume in the material wherein solvent molecules can pass through the loose structure of the bulk material, which can be achieved using certain polymers.[17] Fortunately, mechanically rigid polymers with a high fractional free volume have been studied extensively for applications in gas separations.[17−19] Substituted polyacetylenes, such as poly(1-trimethylsilyl-1-propyne) (PTMSP) and poly(4-methyl-2-pentyne) (PMP), have a carbon backbone with alternating single and double bonds and bulky side groups, resulting in a stiff chain which does not pack well.[19] The result is a rigid polymer with a high fractional free volume which is vapor permeable without being explicitly porous.

TABLE 1. Solubility of Various Vapor Permeable Polymers in Common Solvents. X = Soluble, O = Insoluble

	solubility		
solvent	PDMS	PTMSP	PMP
cyclohexane	0	X	X
toluene	0	X	0
chloroform	0	X	0
tetrahydrofuran	0	X	0
dimethylformamide	0	0	0
methanol	0	0	0
n-heptane	0	X	0
carbon tetrachloride	0	X	X
acetone	0	0	0
methyl ethyl ketone	0	0	0
n-methylpyrrolidone	0	0	0
refs	22	23−26	20

In fact, the vapor permeability for these materials is higher than PDMS for many common gases.[18] PMP, the structure of which is shown in Figure 2, is particularly interesting as this polymer consists exclusively of carbon and hydrogen atoms, giving the polymer a high degree of thermal stability, resistance against a large variety of solvents, and a low surface energy that prevents fouling and allows for simple release of the patterned material when used as a template.[20,21] The resistance of this polymer to solvent commonly used in nanoparticle or polymer inks is greater than the higher-permeability PTMSP, but slightly less than the commonly used PDMS, as shown in Table 1. The polymer has no glass transition temperature, enabling its usage at elevated temperatures, and is optically transparent, allowing registration by optical alignment.

PMP SYNTHESIS, CHARACTERIZATION, AND TEMPLATE CASTING

Poly(4-methyl-2-pentyne) was synthesized following the method of Morisato *et al.*[20] The structure of

TABLE 2. Permeabilities of PDMS and PMP to Some Common Gasses

	gas permeability (barrer)	
gas	PDMS	PMP
H_2	890	5800
N_2	400	1300
O_2	800	2700
CO_2	3800	11000
CH_4	1200	2900
C_2H_6	3300	3700
C_3H_8	4100	7300
n-C_4H_{10}	16000	26000
ref	29,30	31

TABLE 3. Permeabilities of PDMS and PMP to Some Common Solvents

	solvent permeability ($\times 10^{-7}$ g cm/s cm^2)	
solvent	PDMS	PMP
acetone (23 °C)	23.1	14.1
NMP (75 °C)	10.9	5.2
terpineol (75 °C)	5.9	2.6

the synthesized polymer was confirmed using FT-IR spectroscopy, and the resulting spectrum, shown in Figure 2, matches well to those reported in the literature.[20,27] The cast PMP polymer had a measured density of 0.73 ± 0.09 g/cm^3 and a water contact angle of approximately 105°, which is similar to that found in previous works.[27,28] The modulus of elasticity for the PMP was determined to be 1.6 ± 0.3 GPa. For comparison, the modulus of elasticity of the PDMS was measured to be only 950 ± 70 kPa, a difference of 3 orders of magnitude.

The permeabilities of PMP to a variety of common gases and solvents are given in Tables 2 and 3. The gas permeability, which can be important to the release of trapped gases and solvent vapors in nanoimprint or gravure processes, is higher than PDMS for all common gases. The solvent permeability, which was measured by monitoring the mass loss of solvent through the membrane of interest from a closed container, is similar but only slightly less than PDMS for the solvents used in subsequent experiments. These results show that neither solvent nor gas permeability is substantially affected by using PMP instead of PDMS in the patterning templates.

PMP templates were created from the synthesized polymer by solvent casting. Standard polymer processing methods, such as injection molding or hot embossing, are not possible with PMP due to the lack of a glass transition temperature; the PMP breaks down before softening. Solvent casting is a viable alternative which, similar to injection molding or embossing,

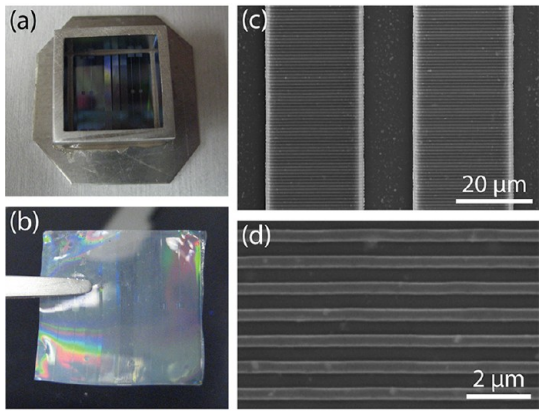

Figure 3. Fabricated PMP templates. Optical images of (a) the master mounted in a casting ring, and (b) the released PMP mold after solvent casting. SEM micrograph of a PMP template, showing (c) microchannels with nanochannels branching off, and (d) a close-up view of the nanochannels.

allows multiple templates to be created from a single master, reducing the cost per template. The PMP films were then mounted on PDMS backings, using only the natural van der Waals forces for adhesion, allowing for easy handling and an even distribution of pressure across the PMP films when pressing into the substrate during patterning.

Optical and SEM micrographs of the PMP template are shown in Figure 3. The dimensions of the template in the lateral and vertical dimensions were characterized by measuring the ratio of the pitch and height of the both micro- and nanolines on the template to those on the master. The dimensions on the template were found to match those on the master to within the margin of error for the measurement, indicating excellent pattern transfer.

RESULTS AND DISCUSSION

The use of PMP as a template material was demonstrated and characterized by patterning various polymer and nanoparticle inks using the microfluidic molding process.[5] This process, illustrated schematically in Figure 4, relies explicitly on the vapor permeability of the template material, using the evaporation of the solvent through the template as a means of filling template cavities with solute. As a result, high-resolution, three-dimensional patterns of a variety of materials can be created on various substrates in a simple and completely additive manner. Previously, when poly(dimethylsiloxane) (PDMS) was used as a template material, the resolution was limited to approximately 10 μm due to the collapse of smaller features, and features that were successfully patterned often exhibited some distortion of template features.[5] These patterning imperfections are caused by the low modulus of elasticity of the template combined with the pressure applied to the template to ensure good conformal contact with the substrate as well as from the fluid motion through template features.

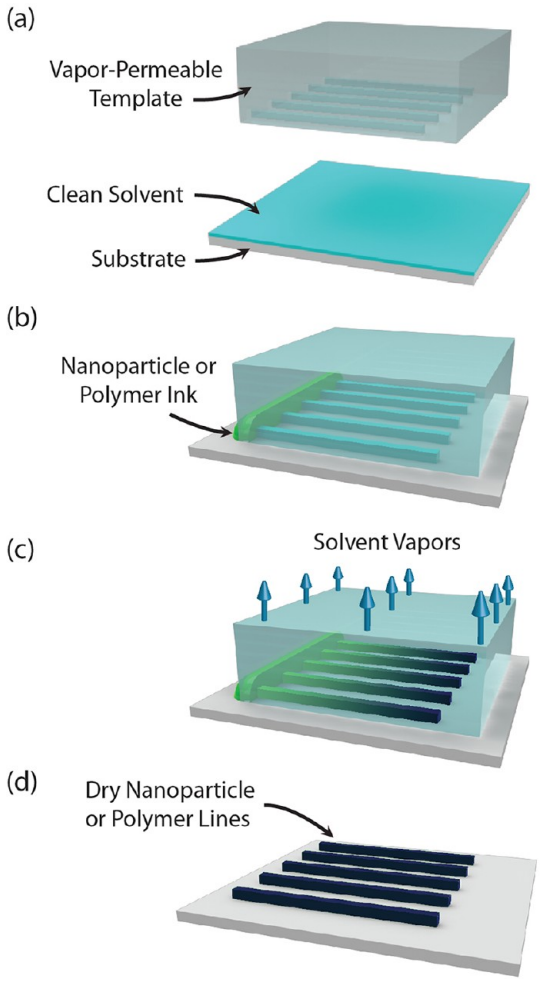

Figure 4. The microfluidic molding patterning process. (a) A vapor-permeable template is pressed into a substrate that is coated in clean solvent. (b) Nanoparticle or polymer ink is applied to the ends of channels. (c) Evaporation of solvent through the template causes the ink to fill the features and concentrate the solutes. (d) When the ink is dry, the template is removed, leaving only the patterned solutes on the substrate.

An initial characterization of the process was performed using cellulose acetate dissolved in acetone at room temperature. A direct comparison of the processing capabilities of the PMP template with the current standard PDMS template was made by patterning similar microscale structures on silicon substrates using each of the two different types of template. The process used for both template materials was identical, except that a higher contact pressure was used for the PMP to ensure good contact with the substrate due to its much higher Young's modulus. That is, the PDMS was held in contact with the substrate with approximately 7 kPa of pressure, and PMP was held with approximately 28 kPa of pressure. The results of the patterning are shown in Figure 5. Feature definition is greatly improved using the PMP templates, which are much better able to retain their shape under the pressures applied to the template during

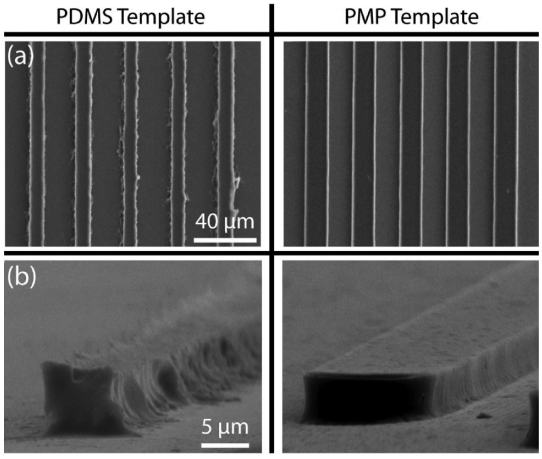

Figure 5. A comparison of features created with PDMS and PMP templates. (a) Lines created with PMP are smoother and straighter with little to no dimensional distortion. (b) The cross sections of features created with PMP are much cleaner, again showing little to no distortion of the template.

patterning due to the higher Young's modulus of the material. The patterning fidelity is improved insofar as the patterns created with the PMP template much better match to the designed patterns on the master. In the cross-section, while the features patterned with the PDMS template show some bowing of the walls and the tops, those patterned with the PMP template have very smooth, vertical sidewalls and flat tops. It is noted that, while the specific deformation is dependent on the specific process used, the properties of the ink being patterned and the designed geometry of template features, the higher Young's modulus of the PMP will always result in higher resolution and patterning fidelity as compared to the more elastic PDMS for a similar set of process conditions.

High resolution and multiscale patterning was also demonstrated using the PMP template material. A master was fabricated which contained 25 μm wide and 2 μm tall lines at a pitch of 50 μm, between which are nanolines with 336 nm width, 840 nm pitch, and 283 nm depth. After patterning, micro- and nanolines were observed to be successfully patterned over a large area. The results are shown in Figure 6a. Both types of lines are patterned simultaneously, despite their very different lateral and vertical dimensions. The dimensions of patterned lines match those of the template to within our measurement uncertainty, indicating proper pattern transfer. It is noted that, compared to PDMS template, the use of PMP templates enables patterning of nanoscale features not normally resolved with PDMS templates while also maintaining a high level of dimensional fidelity on microscale features.

Following initial characterization of the patterning process using cellulose acetate, silver, and gold nanoparticles were patterned. The silver nanoparticles were

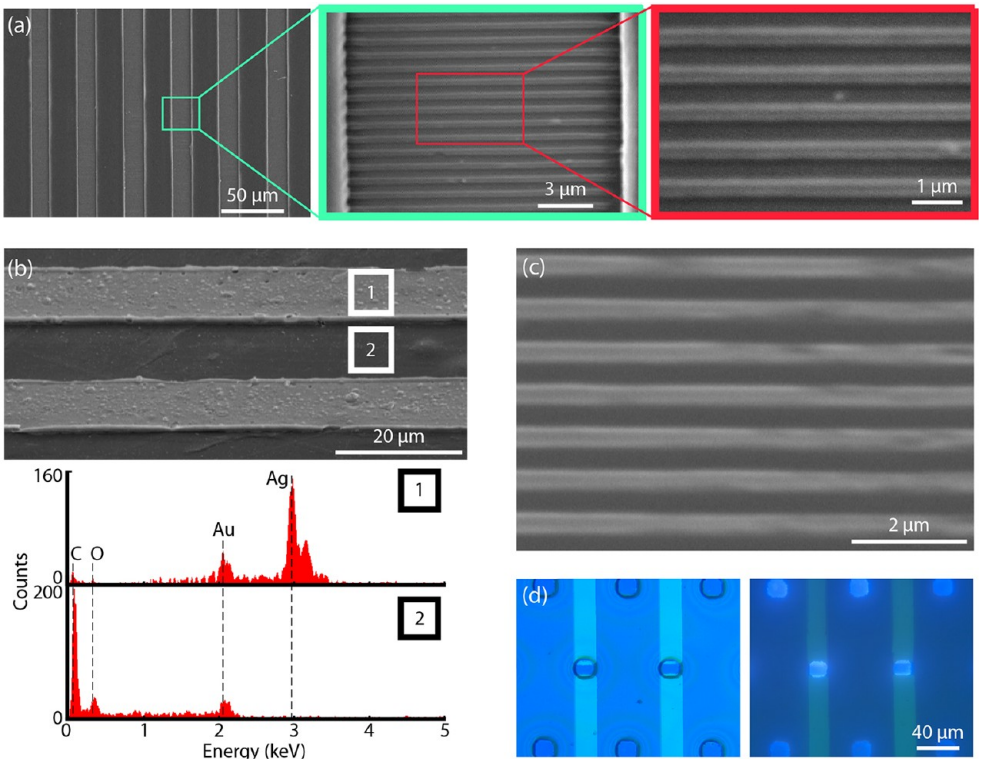

Figure 6. Patterning results using a PMP template. (a) SEM micrographs of multiscale patterns of cellulose acetate on silicon, imaged at a 30° tilt to show the heights of patterned features. (b) SEM micrograph and EDX spectrum of silver nanoparticles patterned on a polyimide substrate. (c) SEM micrograph of gold nanoparticles patterned at high resolution on a silicon substrate. (d) Cellulose acetate patterned on top of gold electrodes (left) and the resulting zinc oxide nanoparticle patterns that result after deposition and mechanical lift-off (right).

encapsulated in a hexanethiol monolayer and suspended in toluene, while the gold nanoparticles are encapsulated in a hexanethiol monolayer and suspended in alpha-terpineol. The silver nanoparticles were patterned into microlines on a polyimide substrate at room temperature. A thin layer of gold was sputtered on the resulting patterns to allow for SEM imaging of the lines on the polymer substrate, and energy-dispersive X-ray spectroscopy (EDX) was used to characterize the patterning. The results are shown in Figure 6b. Strong peaks of silver and gold are seen in the patterned areas, resulting from the nanoparticles and the thin layer of gold used for imaging, with small peaks of carbon and oxygen resulting from the hexanethiol monolayer and polyimide substrate. Only carbon, oxygen, and gold are detected between the patterned lines, and no trace of silver is observed. This analysis indicates that no residual layer is formed between patterned lines in the PMP template, and a good seal formed between the PMP and the substrate despite the increase in Young's modulus of the polymer as compared to PDMS templates.

Gold nanoparticles were patterned on a silicon substrate into nanolines having a width of 314 nm and a pitch of 810 nm, as shown in Figure 6c. The patterning was done at a temperature of 90 °C to facilitate evaporation of the solvent. The results were similar to those of the cellulose acetate patterns created previously, showing that release of higher resolution nanoparticle features is indeed possible using this template material. However, the heights of the gold nanoparticle features show some slight variation along the length of lines, which could be due to oxidation of the hexanethiol monoloayer on the particles and some resulting reflow of the material in the template due to capillary forces and the corresponding reduction in volume. The ratio of the height of the gold nanolines to the measured height of the template used in patterning was 0.85 $\pm$ 0.05, indicating that some volume shrinkage did indeed occur. Since this volume reduction occurs while the template is still in place, the side walls remain straight and only the vertical dimension is reduced. The nonuniformity of the height is suspected to be the result of a Plateau-Rayleigh instability that forms as the vertical dimension is reduced. The distance between peaks of this waviness were measured, and it was found that the wavelength was 1.4 $\pm$ 0.5 μm. This is similar to the calculated wavelength at which instabilities would grow fastest, which is calculated to be 1.38 μm for lines of these dimensions.[32] The results for the silver and gold nanoparticles suggests that proper release of nanoparticle features does occur with PMP templates, enabling the use of this material with a wide variety of polymer and nanoparticle inks.

Finally, the ability to create multilevel patterning was demonstrated by patterning zinc oxide nanoparticles on top of previously defined gold electrodes, using a mechanical lift-off process demonstrated previously.[33] Breifly, the zinc oxide nanoparticle patterns were made by patterning a perforated cellulose acetate sheet using the method described above, depositing zinc oxide nanoparticles into the patterned perforations using the natural evaporation of a sessile droplet, and removing the weakly adhered cellulose acetate sheet mechanically using crepe paper masking tape, leaving the nanoparticle patterns behind. The alignment between the PMP template and the gold electrodes was done using a press consisting of precision vertical and horizontal alignment stages together with an optical microscope with a long working distance. The alignment was done through the optically transparent PMP template, which was mounted on PDMS and adhered to glass by van der Waals forces. Unlike the process described previously, the more rigid PMP template was used as the template material, rather than the rubbery PDMS, allowing the template to be aligned to the substrate much more easily and eliminating the Poisson expansion of the template with applied pressure. Quantitatively, the lateral strain ε' can be expressed as

$$\varepsilon' = -\frac{\nu\sigma}{E} \quad (1)$$

where ν is the Poisson ratio, σ is the applied stress, and E is the Young's modulus. Since the Poisson ratio is of the same order of magnitude for both PDMS and PMP and the Young's modulus of PMP is 3 orders of magnitude higher than PDMS, the lateral strain is substantially reduced for a given applied stress resulting in substantially easier alignment over larger template areas. Experimentally, the patterned cellulose acetate sheet and the final zinc oxide nanoparticle patterns are shown in Figure 6d, showing that good alignment was in fact achieved.

CONCLUSIONS

Poly(4-methyl-2-pentyne) is an extremely suitable material for use as a template for high resolution, large area, three-dimensional patterning of nanoparticles and polymers with alignment. The high vapor-permeability greatly simplifies large-area and high-rate nonphotolithographic patterning processes by allowing for a very straightforward and versatile method for changing ink rheology inside of the template by simple evaporation. Additionally, the mechanical rigidity, thermal and chemical stability, and optical transparency are ideal for creating high quality patterns. In this work, this material was used to pattern both nanoparticles and polymers, achieving a resolution of less than 350 nm with very high patterning fidelity. The patterned features had very straight lines with smooth and vertical sidewalls and good registration capability. The properties of this polymer are highly amenable for future deployment as next generation templates for use in a variety of other patterning technologies, such as gravure, nanoimprint, micromolding in capillaries, and solvent-assisted and solvent absorption micromolding.

METHODS

To synthesize the poly(4-methyl-2-pentyne) (PMP), a catalyst solution was created by combining niobium pentachloride (0.264 g) with triphenyl bismuth (0.428 g) in toluene (21.6 mL) and stirring for 10 min at 90 °C in a nitrogen environment. A monomer solution was created by combining 4-methyl-2-pentyne (2 g) in toluene (2.8 mL). The monomer solution was added dropwise to the catalyst solution and reacted for 1 h at 90 °C. The resulting gel was washed in methanol (40 mL) to remove excess catalyst solution and unreacted monomer, filtered to recover the polymer, and dried under vacuum. The polymer was dissolved in cyclohexane (200 mL), reprecipitated in methanol and filtered, twice, to separate the catalysts, unreacted monomers, and oligomers from the polymer. The resulting polymer was dissolved in cyclohexane (120 mL) and filtered once more to remove any dust or debris. The resulting solution was measured to be approximately 1%, and the polymerization yield was therefore approximately 63%.

To create templates from PMP, the polymer in solvent was poured over a silicon template affixed onto an aluminum casting ring with epoxy. A 1 cm thick PDMS gasket was placed over the casting ring and held in place with a custom-built acrylic clamp to control the evaporation rate of the cyclohexane. The cyclohexane was allowed to evaporate slowly at room temperature for approximately 96 h, after which the PMP templates were gently removed by pulling with tweezers.

To create PDMS templates, poly(dimethylsiloxane) (Sylgard 185-Dow) prepolymer and cross-linker were mixed in a 10:1 ratio, poured over the silicon master and cured on a hot plate at 65 °C for 1 h.

SEM images of the polymer and patterned features were obtained by first sputtering a thin layer of gold on top of any samples containing polymer using a Polaron SEM Coating System. The images were obtained using a Hitachi S-2460N SEM. Dimensions were measured from the images using Adobe Illustrator CS3 software. Multiple measurements were averaged, and the standard deviation of these measurements was taken as the uncertainty.

FT-IR spectra of the synthesized polymer were obtained using a Thermo Nicolet Nexus 870 with Continuum XL IR Microscope.

The modulus of elasticity of the PMP was measured by deflecting a cantilever beam of the PMP polymer mounted on a rigid support with a second cantilever of polyimide with known modulus of elasticity mounted on a moving stage and measuring the ratio of the displacement at the point of contact between the two beams to the applied displacement.

Energy-dispersive X-ray spectroscopy (EDX) was performed using a Kevex Sigma KS2 inside of the Hitachi S-2460N SEM.

Conflict of Interest: The authors declare no competing financial interest.

Acknowledgment. The authors would like to thank H. Pan and C. Grigoropoulos for providing gold and silver nanoparticles. This work was supported by NSF Grant CMMI-0825189.

REFERENCES AND NOTES

1. Ko, S. H.; Park, I.; Pan, H.; Grigoropoulos, C. P.; Pisano, A. P.; Luscombe, C. K.; Frechet, J. M. J. Direct Nanoimprinting of Metal Nanoparticles for Nanoscale Electronics Fabrication. *Nano Lett.* **2007**, *7*, 1869–1877.
2. Kim, E.; Xia, Y. N.; Whitesides, G. M. Polymer Microstructures Formed by Molding in Capillaries. *Nature* **1995**, *376*, 581–584.
3. Kim, E.; Xia, Y. N.; Zhao, X. M.; Whitesides, G. M. Solvent-Assisted Microcontact Molding: A Convenient Method for Fabricating Three-Dimensional Structures on Surfaces of Polymers. *Adv. Mater.* **1997**, *9*, 651–654.
4. Kim, Y. S.; Suh, K. Y.; Lee, H. H. Fabrication of Three-Dimensional Microstructures by Soft Molding. *Appl. Phys. Lett.* **2001**, *79*, 2285–2287.
5. Demko, M. T.; Cheng, J. C.; Pisano, A. P. High-Resolution Direct Patterning of Gold Nanoparticles by the Microfluidic Molding Process. *Langmuir* **2010**, *26*, 16710–16714.
6. Schmid, H.; Michel, B. Siloxane Polymers for High-Resolution, High-Accuracy Soft Lithography. *Macromolecules* **2000**, *33*, 3042–3049.
7. Choi, S. J.; Yoo, P. J.; Baek, S. J.; Kim, T. W.; Lee, H. H. An Ultraviolet-Curable Mold for Sub-100-nm Lithography. *J. Am. Chem. Soc.* **2004**, *126*, 7744–7745.
8. Csucs, G.; Kunzler, T.; Feldman, K.; Robin, F.; Spencer, N. D. Microcontact Printing of Macromolecules with Submicrometer Resolution by Means of Polyolefin Stamps. *Langmuir* **2003**, *19*, 6104–6109.
9. Pisignano, D.; D'Amone, S.; Gigli, G.; Cingolani, R. Rigid Organic Molds for Nanoimprint Lithography by Replica Molding of High Glass Transition Temperature Polymers. *J. Vac. Sci. Technol. B* **2004**, *22*, 1759–1763.
10. Kim, Y. S.; Lee, H. H.; Hammond, P. T. High Density Nanostructure Transfer in Soft Molding using Polyurethane Acrylate Molds and Polyelectrolyte Multilayers. *Nanotechnology* **2003**, *14*, 1140–1144.
11. Khang, D. Y.; Kang, H.; Kim, T.; Lee, H. H. Low-Pressure Nanoimprint Lithography. *Nano Lett.* **2004**, *4*, 633–637.
12. Williams, S. S.; Retterer, S.; Lopez, R.; Ruiz, R.; Samulski, E. T.; DeSimone, J. M. High-Resolution PFPE-based Molding Techniques for Nanofabrication of High-Pattern Density, Sub-20 nm Features: A Fundamental Materials Approach. *Nano Lett.* **2010**, *10*, 1421–1428.
13. Lee, B. K.; Hong, L.-Y.; Lee, H. Y.; Kim, D.-P.; Kawai, T. Replica Mold for Nanoimprint Lithography from a Novel Hybrid Resin. *Langmuir* **2009**, *25*, 11768–11776.
14. Lee, B. K.; Cho, H.; Chung, B. H. Nonstick, Modulus-Tunable and Gas-Permeable Replicas for Mold-Based, High-Resolution Nanolithography. *Adv. Funct. Mater.* **2011**, *21*, 3681–3689.
15. Chou, S. Y.; Krauss, P. R.; Renstrom, P. J. Imprint of Sub-25 Nm Vias and Trenches in Polymers. *Appl. Phys. Lett.* **1995**, *67*, 3114–3116.
16. Puetz, J.; Aegerter, M. A. Direct Gravure Printing of Indium Tin Oxide Nanoparticle Patterns on Polymer Foils. *Thin Solid Films* **2008**, *516*, 4495–4501.
17. Pandey, P.; Chauhan, R. S. Membranes for Gas Separation. *Prog. Polym. Sci.* **2001**, *26*, 853–893.
18. Robeson, L. M. Polymer Membranes for Gas Separation. *Curr. Opin. Solid State Mater. Sci.* **1999**, *4*, 549–552.
19. Budd, P. M.; McKeown, N. B. Highly Permeable Polymers for Gas Separation Membranes. *Polym. Chem.* **2010**, *1*, 63–68.
20. Morisato, A.; Pinnau, I. Synthesis and Gas Permeation Properties of Poly(4-methyl-2-pentyne). *J. Membr. Sci.* **1996**, *121*, 243–250.
21. Shao, L.; Samseth, J.; Hagg, M. B. Crosslinking and Stabilization of Nanoparticle Filled PMP Nanocomposite Membranes for Gas Separations. *J. Membr. Sci.* **2009**, *326*, 285–292.
22. Lee, J. N.; Park, C.; Whitesides, G. M. Solvent Compatibility of Poly(dimethylsiloxane)-Based Microfluidic Devices. *Anal. Chem.* **2003**, 75.
23. Bi, J.; Simon, G. P.; Yamasaki, A.; Wang, C. L.; Kobayashi, Y.; Griesser, H. J. Effects of Solvent in the Casting of Poly-(1-trimethylsilyl-1-propyne) Membranes. *Radiat. Phys. Chem.* **2000**, *58*, 563–566.
24. Claes, S.; Vandezande, P.; Mullens, S.; Adriaensens, P.; Peeters, R.; Maurer, F. H.; Bael, M. K. V. Crosslinked Poly[1-(trimethylsilyl)-1-propyne] Membranes: Characterization and Pervaporation of Aqueous Tetrahydrofuran Mixtures. *J. Membr. Sci.* **2012**, *389*, 459–469.
25. Feron, P. H. M.; Volkov, V. V.; Khotimsky, V. S.; Teplyakov, V. V. Membrane Gas Separation. US Patent 7,591,878, September 22, 2009.
26. Volkov, A. V.; Parashchuk, V. V.; Stamatialis, D. F.; Khotimsky, V. S.; Volkov, V. V.; Wessling, M. High Permeable PTMSP/PAN Composite Membranes for Solvent Nanofiltration. *J. Membr. Sci.* **2009**, *333*, 88–93.
27. Masuda, T.; Kawasaki, M.; Okano, Y.; Higashimura, T. Polymerization of Aliphatic Acetylenes —Polymerization of Methylpentynes by Transition-Metal Catalysts—Monomer Structure, Reactivity, and Polymer Properties. *Polym. J.* **1982**, *14*, 371–377.
28. Shao, L.; Samseth, J.; Hagg, M. B. Effect of Plasma Treatment on the Gas Permeability of Poly(4-methyl-2-pentyne) Membranes. *Plasma Process. Polym.* **2007**, *4*, 823–831.
29. Merkel, T. C.; Bondar, V. I.; Nagai, K.; Freeman, B. D.; Pinnau, I. Gas Sorption, Diffusion, and Permeation in Poly-(dimethylsiloxane). *J. Polym. Sci., Polym. Phys.* **2000**, *38*.
30. Raharjo, R. D.; Freeman, B. D.; Paul, D. R.; Sarti, G. C.; Sanders, E. S. Pure and Mixed Gas CH_4 and n-C_4H_{10} Permeability and Diffusivity in Poly(dimethylsiloxane). *J. Membr. Sci.* **2007**, *306*, 75–92.
31. Toy, L. G.; Nagai, K.; Freeman, B. D.; Pinnau, I.; He, Z.; Masuda, T.; Teraguchi, M.; Yampolskii, Y. P. Pure-Gas and Vapor Permeation and Sorption Properties of Poly-[1-phenyl-2-[p-(trimethylsilyl)phenyl]acetylene] (PTMSDPA). *Macromolecules* **2000**, *33*, 2516–2524.
32. de Gennes, P.-G.; Brochard-Wyart, F.; Quere, D. *Capillarity and Wetting Phenomena: Drops, Bubbles, Pearls, Waves*; Springer: New York, 2004; p 120.
33. Demko, M. T.; Choi, S.; Zohdi, T. I.; Pisano, A. P. High Resolution Patterning of Nanoparticles by Evaporative Self-Assembly Enabled by *in Situ* Creation and Mechanical Lift-Off of a Polymer Template. *Appl. Phys. Lett.* **2011**, *99*, 253102.